Detection of ozone on Saturn's satellites Rhea and Dione

K. S. Noll*, T. L. Roush†‡, D. P. Cruikshank†, R. E. Johnson§ & Y. J. Pendleton†

* *Space Telescope Science Institute, 3700 San Martin Drive, Baltimore, Maryland 21218, USA*
† *NASA Ames Research Center, Moffett Field, California 94035, USA*
‡ *Department of Geosciences, San Francisco State University, San Francisco, California 94132, USA*
§ *University of Virginia, Engineering Physics, Charlottesville, Virginia 22901, USA*

The satellites Rhea and Dione orbit within the magnetosphere of Saturn, where they are exposed to particle irradiation from trapped ions. A similar situation applies to the galilean moons Europa, Ganymede and Callisto, which reside within Jupiter's radiation belts. All of these satellites have surfaces rich in water ice[1,2]. Laboratory studies of the interaction of charged-particle radiation with water ice predicted[3] the tenuous oxygen atmospheres recently found on Europa[4] and Ganymede[5]. However, theoretical investigations did not anticipate the trapping of significantly larger quantities of O_2 within the surface ice[6]. The accumulation of detectable abundances of O_3, produced by the action of ultraviolet or charged-particle radiation on O_2, was also not predicted before being observed on Ganymede[7]. Here we report the identification of O_3 in spectra of the saturnian satellites Rhea and Dione. The presence of trapped O_3 is thus no longer unique to Ganymede, suggesting that special circumstances may not be required for its production.

The observations of Rhea, Dione and Iapetus reported here (Fig. 1) were obtained with the Hubble Space Telescope's Faint Object Spectrograph (Table 1). The data were reduced using the standard procedures maintained by the Space Telescope Science Institute. Geometric albedos were calculated by dividing out the solar spectrum[8] and by correcting to zero degrees phase angle[9,10].

The spectra of both hemispheres of Rhea and Dione show clear minima at 260 ± 5 nm. The Iapetus spectra have shallow minima at 270 ± 10 nm (trailing hemisphere) and 255 ± 10 nm (leading hemisphere). Of the products that can be produced in H_2O ice either by radiolysis or photolysis, only O_3 has an absorption feature near 260 nm (refs 11, 12). The wavelength of the albedo minimum is an excellent match to the wavelength of the feature observed on Ganymede's trailing hemisphere[7]. The inferred O_3/O_2 ratio on Ganymede is close to that expected for equilibrium gas trapped in voids or defects in the ice[7,13], adding confidence in the identification of the 260-nm absorber as O_3. Due to the similar surfaces and charged particle fluxes on Rhea and Dione, we identify the Hartley continuum of O_3 with the 260-nm absorption on these satellites. The weakness or absence of the feature on Iapetus is consistent with the lower charged-particle density in the solar wind at Iapetus compared to that found in Saturn's magnetosphere at the radii of Rhea and Dione's orbits. Smaller amounts of O_2 and O_3 are therefore expected in the ice on Iapetus.

To estimate the amount of O_3 in the observed spectra of Rhea, Dione and Iapetus we produced a series of models which tested a range of assumptions concerning the continuum. We find the column abundance of ozone to be $N(O_3) = (1–6) \times 10^{16}$ cm^{-2} for Rhea's leading hemisphere with comparable values for the trailing hemisphere and for both hemispheres of Dione. For Iapetus's icy trailing hemisphere we find $N(O_3) < 0.5 \times 10^{16}$ cm^{-2} with a poor match to the wavelength of the spectral minimum. Absorption coefficients of ozone were calculated from a gas-phase spectrum which was shifted by +6 nm (ref. 14) and broadened to a full-width at half-maximum intensity of 80 nm (ref. 15). Though these effects are observed in the laboratory, there are no measurements of O_3 absorption under conditions similar to those found on the satellites of Saturn and Jupiter, and this remains a continuing source of uncertainty in our estimates of O_3 abundances. However, unless the Hartley continuum of O_3 is significantly broader at 100 K than it is at 77 K, O_3 cannot account for the bulk of the ultraviolet absorption; some other absorber is required. The model shown in Fig. 2 uses a continuum that includes absorption by small amounts of organic residue created by irradiation of water ice and ethane[16] and an additional, linear slope at wavelengths less than 477 nm. We have assumed that the organic residue produced in the laboratory is similar to what might be produced in any icy surface with small quantities of carbon-containing material. The additional slope is needed to match the continued red slope observed at wavelengths <220 nm in the spectrum of Rhea's trailing hemisphere and may be related to the observation that spectral slopes in this part of the spectrum for residues created by irradiation of ice mixtures are dependent on radiation history[17]. With this continuum we find $N(O_3) = 2 \times 10^{16}$ cm^{-2}. The uncertainties in this estimate are at least a factor of 3.

Table 1 HST observations of Saturn's satellites

Satellite	Date (UT)	λ (nm)	θ (deg)	α (deg)
Dione (T)	21 Dec. 96	220–480	264	5.9
(L)	28 Nov. 96	220–480	89	5.4
Rhea (T)	23 Oct. 94	190–330	288	4.7
(L)	27 Nov. 96	220–480	95	5.4
Iapetus (T)	22 Oct. 94	190–330	269	4.7
(L)	03 Jan. 96	190–330	91	5.5

λ, wavelength; θ, orbital longitude; α, phase angle; T, trailing hemisphere; L, leading hemisphere.

Ozone is produced in ice by a chain of events starting with the dissociation of H_2O by high-energy charged-particle impacts. Oxygen and hydrogen produced in this way recombine, producing some O_2 and H_2. The H_2 subsequently escapes from the satellite because of its high mobility in an ice lattice and its low mass. Oxygen molecules that remain trapped in the ice are exposed to ultraviolet radiation where an equilibrium between O_2 and O_3 results. If our understanding of the production of O_3 is correct, the presence of O_3 on these satellites implies that O_2 is also present at abundances of the order of 500 times higher than O_3 (refs 7, 13). At sufficiently high density and low temperature[15], pairs of O_2 molecules absorb in a series of weak bands, most easily observed at 580 and 630 nm (ref. 6). The inferred abundance of O_3 on Rhea and Dione is approximately half that found on Ganymede which might lead to O_2 bands with a maximum absorption of 1% of the continuum. Visible-wavelength spectra of the precision needed to identify these weak O_2 bands have not been published for Saturn's satellites, but could be obtained with current technology. The lack of these features would not rule out O_3, but their presence would be strong additional evidence for its presence. Another test would be to search for O_3 on the icy satellites Tethys and Enceladus which orbit Saturn at a distance where the density of charged particles is significantly higher than at Rhea or Dione[3]. If the total flux of charged particles is the most important factor in the production of O_3, then we expect O_3 to be present on both Tethys and Enceladus. The satellites of Uranus are also ice-rich objects[18], but experience a much lower charged-particle flux than Rhea[3] and appear to have carbon contaminants which could compete for oxygen. As a results, we expect a lower abundance of O_3 on these satellites.

The rotation periods of Rhea, Dione and Iapetus are synchronous with their revolution about Saturn so that one hemisphere (leading) always faces in the direction of orbital motion while the opposite (trailing) faces away. Both charged-particle radiation

and micrometeorite impacts can have asymmetric effects on the surfaces, with a higher flux of charged particles striking trailing hemispheres and micrometeorite impacts predominating on the leading hemispheres of the satellites[19]. Jupiter's icy satellites, also in synchronous rotation, show many leading–trailing hemisphere dichotomies[1,19], most of which are attributable to irradiation of the trailing hemisphere. Saturn's satellites Rhea and Dione exhibit leading–trailing hemisphere differences in colour, albedo[20] and ice-band depth[2], and experience charged-particle fluxes comparable to Ganymede[3]. Iapetus is marked by an extreme darkening of its leading hemisphere but orbits outside Saturn's magnetosphere where it encounters the lower-density charged-particle environment of the solar wind. Besides changes in albedo, colour and grain properties, Europa, Ganymede and Callisto each have compositional differences between leading and trailing hemispheres. However, the compositional differences defy a single explanation with excesses of SO_2 on Europa's trailing hemisphere[21,22], O_2 and O_3 on Ganymede's trailing hemisphere[6,7], and SO_2 on Callisto's leading hemisphere[23]. All three of Jupiter's icy satellites show evidence of excess oxygen being produced in the surface ices, though it appears that when sulphur is present in the ice it competes effectively for the oxygen and limits the production of O_3. The origin of the sulphur may either be external or may be related to the fraction of non-ice components present on the surfaces of Jupiter's icy satellites[1,22,23]. Although there is circumstantial evidence linking changes in albedo and spectrophotometric properties of Jupiter's satellites to the observed hemispheric compositional differences, a common causal connection has not been established. Saturn's satellites are smaller than Jupiter's and the surfaces are nearly pure water ice[2]; these two significant differences may constrain the conditions under which O_3 is formed and determine if spectrophotometric and compositional changes can be related.

Ozone appears to be present at a similar abundance on both leading and trailing hemispheres of Rhea and Dione. The trailing hemispheres of both satellites have lower albedos than their leading hemispheres, but the difference between the albedo in the ultraviolet absorption feature at 260 nm and the albedo in the visible wavelength continuum at 600 nm is very similar, 0.3–0.35 albedo units. Differences in albedo at visible wavelengths between leading and trailing hemispheres of Rhea and Dione must be related to the presence of small quantities of non-ice materials such as organic residues or minerals that will also absorb at ultraviolet wavelengths. A natural explanation of the apparent similarity in the shape of the feature would arise if the surfaces could be described as areal mixtures of spectrally distinct material. The similarity of the O_3 absorption depths on both hemispheres of Rhea and Dione requires that the charged particles initiating O_2 and O_3 production have energies sufficiently high that their incidence on the surface is nearly isotropic. It has been shown that 20-keV oxygen ions will strike Dione nearly isotropically whereas colder oxygen ions (0.2-keV) do not[24], possibly indicating a minimum required energy for obtaining a measurable quantity of O_3. The energy of an ion with a gyroradius equal to the satellite radius is 43 times higher for Ganymede than for Dione[3], a fact that may account for the apparent difference in longitudinal distribution of O_3 between Dione and Rhea compared to Ganymede.

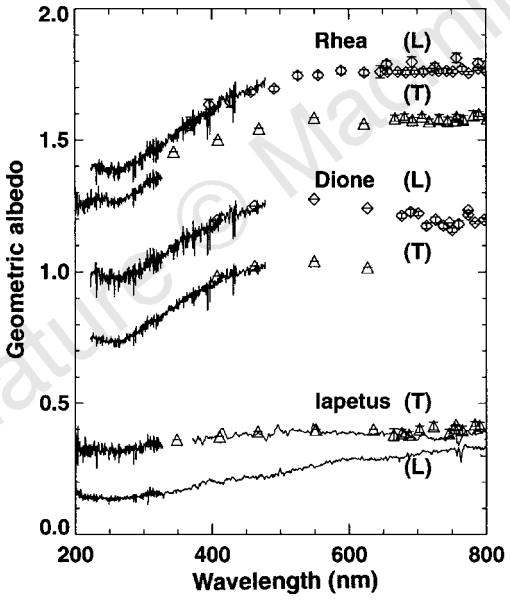

Figure 1 Geometric albedos of Rhea, Dione and Iapetus as a function of wavelength. Spectra of both leading (L) and trailing (T) hemispheres are shown. The thick solid curves are the HST data reported here. Discrete points are from Roush *et al.*[18] from a variety of sources, thin solid curves are scaled reflectances from Vilas *et al.*[29]. Dione albedos are offset by +0.5, Rhea albedos by +1.0, and the spectrum of Iapetus' dark leading hemisphere has been scaled by a factor of 2.5 for clarity. Spectra of Iapetus and Rhea's trailing hemisphere were corrected for scattered light at wavelengths below 220 nm. The correction is small for wavelengths greater than 200 nm. Both hemispheres of Rhea and Dione have pronounced minima at 260 nm. The Iapetus spectra also appear to have weak minima, but at different wavelengths than Rhea and Dione. For Rhea's trailing hemisphere we also obtained data at wavelengths less than 220 nm. The data here suggest that there may be a second minimum at ~210 nm, though the signal-to-noise ratio is too low to be definitive. A similar minimum was noted in Callisto's spectrum[23], but has not been identified.

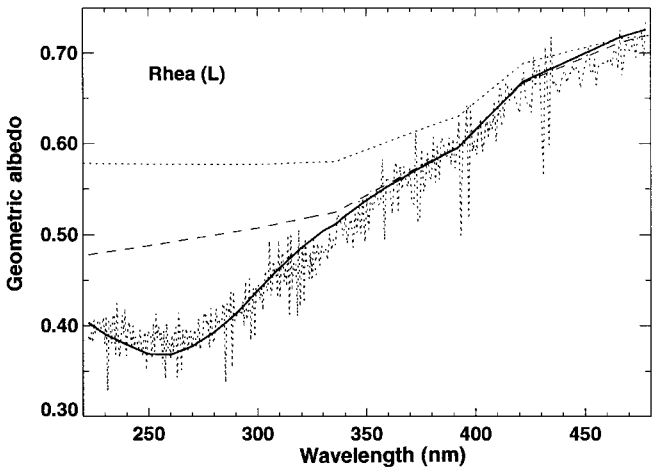

Figure 2 The predictions of a model including O_3 (solid line), plotted with the spectrum of Rhea's leading (L) hemisphere (dotted curve). The continuum consists of a mixture of 97.5% ice and 2.5% organic residues from an irradiated 6 : 1 mixture of H_2O ice and C_2H_6 ice[16] (sometimes called ice tholins, upper dotted line) with an additional constant-slope absorber below 477 nm (dashed line). This added absorption is required both to fit the observed spectrum from 350 to 450 nm and also to account for the fact that at wavelengths below 220 nm the albedo of Rhea's trailing hemisphere remains low. Other mixes of candidate continuum absorbers are also possible, but are not tested in our models.

The detection of O_3 on Rhea and Dione is the first evidence that the accumulation of oxygen and ozone in icy surfaces exposed to ion irradiation may be a widespread process with significance in at least two areas outside the study of the Solar System. Molecular oxygen has been predicted to be abundant in the mantles of interstellar grains in dense clouds[25] and production of O_3 in these grains via irradiation by cosmic rays, stellar winds, or ultraviolet light may be an important factor to consider in models of grain chemistry[11]. Possibly of greater significance, plans to search for and identify Earth-like planets around other stars frequently cite the 9.8-μm band of O_3 as a means to identify planets with massive O_2 atmospheres[26]. A significant component of the Earth's atmosphere was probably derived from impacts of icy comets[27]. If the ices in these comets contain excess oxygen produced by irradiation as the comet accretes, the volatiles delivered to a planetary atmosphere in this way could contain as much as a few per cent O_2 by mass (in excess of the oxygen contained in H_2O ice). Because ozone is a very nonlinear tracer of molecular oxygen in a planetary atmosphere, an Earth-like atmosphere with a partial pressure of O_2 of only 2 mbar, an amount that could conceivably be supplied by O_2-saturated ices, would have a detectable column of O_3 only one-quarter that in Earth's present atmosphere[28] (2 mbar is 2% of Earth's sea-level pressure or ~10% of the O_2 currently in the atmosphere). The identification of oxygen-containing atmospheres on extrasolar planets through detection of O_3 may not, therefore, be an unambiguous way of identifying planets with Earth-like biology. □

Received 27 March; accepted 13 May 1997.

1. Clark, R. N. Ganymede, Europa, Callisto, and Saturn's rings: Compositional analysis from reflectance spectroscopy. *Icarus* **44,** 388–409 (1980).
2. Clark, R. N., Brown, R. H., Owensby, P. D. & Steele, A. Saturn's satellites: Near-infrared spectrophotometry (0.65–2.5 μm) of the leading and trailing sides and compositional implications. *Icarus* **58,** 265–281 (1984).
3. Johnson, R. E. *Energetic Charged Particle Interactions with Atmospheres and Surfaces* (Springer, Berlin, 1990).
4. Hall, D. T., Strobel, D. F., Feldman, P. D., McGrath, M. A. & Weaver, H. A. Detection of an oxygen atmosphere on Jupiter's moon Europa. *Nature* **373,** 677–679 (1995).
5. Barth, C. A. *et al.* Galileo ultraviolet observations of atomic hydrogen in the atmosphere of Ganymede. *Geophys. Res. Lett.* (in the press).
6. Spencer, J. R., Calvin, W. M. & Person, M. J. Charge-coupled device spectra of the galilean satellites: Molecular oxygen on Ganymede. *J. Geophys. Res.* **100,** 19049–19056 (1995).
7. Noll, K. S., Johnson, R. E., Lane, A. L., Domingue, D. & Weaver, H. A. Detection of ozone on Ganymede. *Science* **273,** 341–343 (1996).
8. Woods, T. N., Rottman, G. J. & Ucker, G. J. Solar-stellar irradiance comparison experiment 1: 2. Instrument calibrations. *J. Geophys. Res.* **98,** 10679–10694 (1993).
9. Buratti, B. & Veverka, J. Voyager photometry of Rhea, Dione, Tethys, Enceladus, and Mimas. *Icarus* **58,** 254–264 (1984).
10. Morrison, D., Jones, T. J., Cruikshank, D. P. & Murphy, R. E. The two faces of Iapetus. *Icarus* **24,** 157–171 (1975).
11. Elsila, J., Allamandola, L. J. & Sandford, S. A. The 2140 cm^{-1} (4.673 microns) solid CO band: The case for interstellar ice analogs. *Astrophys. J.* (in the press).
12. Matich, A. J., Bakker, M. G., Lennon, D., Quickenden, T. I. & Freeman, C. G. O_2 luminescence from UV-excited H_2O and D_2O ices. *J. Phys. Chem.* **97,** 10539–10553 (1993).
13. Johnson, R. E. & Jesser, W. A. O_2/O_3 microatmospheres in the surface of Ganymede. *Astrophys. J.* **480,** L79–L82 (1997).
14. Taube, H. Photochemcial reactions of ozone in solution. *Trans. Faraday Soc.* **53,** 656–665 (1956).
15. Vaida, V., Donaldson, D. J., Strickler, S. J., Stephens, S. L. & Birks, J. W. A reinvestigation of the electronic spectra of ozone: Condensed-phase effects. *J. Phys. Chem.* **93,** 506–508 (1989).
16. Khare, B. N. *et al.* Production of optical constants of ice tholin from charged particle irradiation of (1 : 6) C_2H_6/H_2O at 77 K. *Icarus* **103,** 290–300 (1993).
17. Thompson, W. R., Murray, B., Khare, B. N. & Sagan, C. Coloration and darkening of methane clathrate and other ices by charged particle irradiation: Application to the outer solar system. *J. Geophys. Res.* **92,** 14933–14947 (1987).
18. Roush, T. L., Cruikshank, D. P. & Owen, T. C. in *Volatiles in the Earth and Solar System* (ed Farley, K. A.) 143–153 (Am. Inst. Phys., New York, 1995).
19. Buratti, B. Ganymede and Callisto: Surface textural dichotomies and photometric analysis. *Icarus* **92,** 312–323 (1991).
20. Buratti, B., Mosher, J. A. & Johnson, T. V. Albedo and color maps of the saturnian satellites. *Icarus* **87,** 339–357 (1990).
21. Lane, A. L., Nelson, R. M. & Matson, D. L. Evidence for sulphur implantation in Europa's UV absorption band. *Nature* **292,** 38–39 (1981).
22. Noll, K. S., Weaver, H. A. & Gonnella, A. M. The albedo spectrum of Europa from 2200 Å to 3300 Å. *J. Geophys. Res.* **100,** 19057–19059 (1995).
23. Noll, K. S., Johnson, R. E., McGrath, M. & Caldwell, J. J. Detection of SO_2 on Callisto with the Hubble Space Telescope. *Geophys. Res. Lett.* **24,** 1139–1142 (1997).
24. Pospieszalska, M. K. & Johnson, R. E. Magnetospheric ion bombardment profiles of satellites: Europa and Dione. *Icarus* **78,** 1–13 (1989).
25. Tielens, A. G. G. M. & Hagen, W. Model calculations of the molecular composition of interstellar grain mantles. *Astron. Astrophys.* **114,** 245–260 (1982).
26. Burke, B. F. Detection of planetary systems and the search for evidence of life. *Nature* **322,** 340–341 (1986).
27. Owen, T., Bar-Nun, A. & Kleinfeld, I. Possible cometary origin of heavy noble gases in the atmospheres of Venus, Earth and Mars. *Nature* **358,** 43–46 (1992).
28. Léger, A., Pirre, M. & Marceau, F. J. Relevance of oxygen and ozone detections in the search for primitive life in extrasolar planets. *Adv. Space Res.* **14,** 117–122 (1994).
29. Vilas, F., Larson, S. M., Stockstill, K. R. & Gaffey, M. J. Unraveling the zebra: Clues to the Iapetus dark material composition. *Icarus* **124,** 262–267 (1996).

Acknowledgements. We thank M. J. Bartholomew for sharing her models of visible and IR satellite spectra on which our models of the UV spectrum are based. This work was supported by the Space Telescope Science Institute, which is operated by the Association of Universities for Research in Astronomy, Inc., under NASA contract.

Correspondence should be addressed to K.S.N.

Modelling the evolution of human trail systems

Dirk Helbing*, Joachim Keltsch† & Péter Molnár‡

** Institute of Theoretical Physics, University of Stuttgart, Pfaffenwaldring 57/III, 70550 Stuttgart, Germany*
† Science–Computing, Hagellocher Weg 71, 72070 Tübingen, Germany
‡ Center for Theoretical Studies of Physical Systems, Clark Atlanta University, James P. Brawley Drive, Atlanta, Georgia 30314, USA

Many human social phenomena, such as cooperation[1–3], the growth of settlements[4], traffic dynamics[5–7] and pedestrian movement[7–10], appear to be accessible to mathematical descriptions that invoke self-organization[11,12]. Here we develop a model of pedestrian motion to explore the evolution of trails in urban green spaces such as parks. Our aim is to address such questions as what the topological structures of these trail systems are[13], and whether optimal path systems can be predicted for urban planning. We use an 'active walker' model[14–19] that takes into account pedestrian motion and orientation and the concomitant feedbacks with the surrounding environment. Such models have previously been applied to the study of complex structure formation in physical[14–16], chemical[17] and biological[18,19] systems. We find that our model is able to reproduce many of the observed large-scale spatial features of trail systems.

Previous studies have shown that various observed self-organization phenomena in pedestrian crowds can be simulated very realistically. These phenomena include the emergence of lanes of uniform walking direction and oscillatory changes of the passing direction at bottlenecks[7,10]. Another interesting collective effect of pedestrian motion, which we have investigated very recently, is the formation of trail systems in green areas. In many cases, the

Figure 1 Between the straight, paved ways on the university campus in Stuttgart-Vaihingen a trail system has evolved (centre of the picture). Two types of nodes are observed: intersections of two trails running in a straight line and junctions of two trails which smoothly merge into one trail.